Low Power Magnetic Bearing Design For High Speed Rotating Machinery

P. E. Allaire, E. H. Maslen,
and R. R. Humphris,
Department of Mechanical and Aerospace Engineering
University of Virginia
Charlottesville, VA 22901

C. K. Sortore
Aura Systems, Inc.
El Segundo, CA 90245

P. A. Studer
Magnetic Concepts
Silver Springs, MD 20901

SUMMARY

Magnetic suspension technology has advanced to the point of being able to offer a number of advantages to a variety of applications in the rotating machinery and aerospace fields. One strong advantage of magnetic bearings over conventional bearings is the decrease in power consumption. The use of permanent magnets, along with electromagnets, is one appealing option which can further reduce the power consumption of the bearing.

The design and construction of a set of permanent magnet biased, actively controlled magnetic bearings for a flexible rotor is presented. Both permanent magnets and electromagnets are used in a configuration which effectively provides the necessary fluxes in the appropriate air gaps, while simultaneously keeping the undesirable destabilizing forces to a minimum. The design includes two radial bearings and a thrust bearing.

The theoretical development behind the design is briefly discussed. Experimental performance results for a set of operating prototype bearings is presented. The results include measurements of load capacity, bearing stiffness and damping and the dynamic response of the rotor. With few exceptions, the experimental measurements matched very well with the predicted performance. The power consumption of these bearings was found to be significantly reduced from that for a comparable set of all electromagnetic bearings.

INTRODUCTION

Magnetic bearings have a number of strong advantages. One most obvious advantage is their non–contacting, virtually friction–free characteristics. Entire lubrication systems and the need for mechanical oil seals, which add to friction losses and instabilities associated with cross coupled bearing coefficients, can be eliminated by using these types of bearings. The life expectancy of a magnetic bearing, in many cases, can be much higher than that of a conventional bearing. Due to the non–contacting nature of the bearings, mechanical parts do not wear out. This can obviously increase system reliability and decrease costly repairs and necessary maintenance which interrupt profitable machine operation. If designed properly, a magnetic bearing can perform under much harsher conditions and environments for extended periods of time which would not be possible with other types of bearings. One further advantage of the frictionless characteristic of these bearings is that of power loss. The power consumption of a conventional fluid–film bearing is in many cases much more than for a magnetic bearing. Power loss reductions of one order of magnitude or more can be expected when a machine is converted from using conventional bearings to magnetic bearings.

A variety of work has been accomplished on a number of different applications and aspects of magnetic bearings. An extensive amount of research has been performed by a number of university and industry researchers on the development of magnetic bearings in an industrial canned motor pump [1]. A number of other successful industrial applications of magnetic bearings has been reported by Weise [2]. Burrows et. al. [3] presents the development and application of a magnetic bearing specifically designed for the vibration control of a flexible rotor. Keith, et. al. [4] successfully developed a PC–based digital controller for magnetic bearings. Continuing research is being performed in the areas of digital and adaptive controls for magnetic bearings. In researching the use of permanent magnets in combination with electromagnets, of particular interest are two patents credited to Philip Studer [5, 6]. These patents contain a number of features, primarily dealing with permanent magnets, which have useful application to the bearings discussed in this paper. Wilson and Studer [7] have also applied the permanent magnet bias concept to a linear motion bearing. Ohkami et. al. [8] have performed some interesting comparison studies of magnetic bearings of various configurations which use permanent magnets. Another paper by Tsuchiya et. al. [9] studies and comments on the stability of a high speed rotor which is suspended in magnetic bearings biased with permanent magnets. Meeks [10] has also performed a comparison of the various magnetic bearing design approaches and concludes that the combining of actively controlled electromagnets with permanent magnets results in a superior magnetic bearing in terms of size, weight and power consumption. The rare earth permanent magnets of today, in particular Sm–Co and Nd–Fe–Bo magnets, offer very high performance characteristics in terms of magnetic strength, energy product and thermal qualities. The magnet designer is able to concentrate a very large amount of magnetic energy in a small package, making more efficient use of available space.

The design concept for the permanent magnet biased magnetic bearing design discussed in this paper is a variation on research and development reported by Studer [5, 6]. The following two sections give a brief description of how the bearings conceptually operate.

Radial Magnetic Bearing Description

A diagram of a permanent magnet biased radial magnetic bearing is shown in Figure 1. This bearing is designed to operate at one end of the rotor and control radial forces only. Four axially magnetized arc segment magnets are positioned circumferentially adjacent to the stator. The bias flux generated by the permanent magnets passes down the laminated stator pole leg, through the working air gap, axially along the shaft, then returns to the permanent magnet via

a radial bias pole piece. The active control flux generated by the coils also passes down the stator pole leg and through the working air gap. The return path for the active flux is then circumferentially around the stator, as shown in Figure 1. This design requires only four poles and four coils, unlike an all electromagnetic design which generally requires eight. In addition, since the coils for each bearing axis are connected in series, the bearing control system requires only five current amplifier channels, which is half as many as required of the all electromagnetic bearing.

Combination Radial/Thrust Magnetic Bearing Description

A schematic of this bearing design, revealing the various magnetic paths, is shown in Figure 2. This bearing combines control of both radial and thrust forces. The radial portion of the bearing is identical to that which was described in the previous section. The thrust control however, is implemented by a unique magnetic flux configuration. The permanent magnet bias flux passing along the shaft splits equally between the two thrust poles before returning to the permanent magnet. A single active coil produces a magnetic flux, in the shape of a toroid, which symmetrically adds or subtracts to the bias flux in the working air gaps between the thrust disk and thrust poles.

Design Concept

The bearings designed for this project are different from all electromagnetic bearing designs in that they employ both permanent magnets and electromagnets. Permanent magnets generate the bias flux in the working air gaps and electromagnets are used to modulate this flux.

The purpose of establishing a bias flux in the working air gaps is to linearize the governing force equation of the magnetic actuator. The bias flux is a nominal flux density about which the control flux is varied. If a bias flux of zero is used, (only one opposing actuator is operated at a time,) then the force generated by the actuator on the rotor follows a quadratic force law, i.e., the force will be proportional to the square of the flux density in the air gaps. Consequently, the force slew rate will be zero when the rotor is in the nominal balanced position and the transient response will be adversely effected. If, however, the bearing fluxes are modulated about a non–zero bias flux, (with opposing actuators symmetrically perturbed,) it is easily shown that the force becomes linearly related to the control flux. The following section demonstrates this important relation.

Force Relationships

The force generated in an air gap of area A_g and length $_g$ by a magnetic actuator can be expressed by the direct relation

$$F = \frac{1}{2\mu_0}(B_g)^2 A_G \qquad (1)$$

where B_g is the flux density in the air gap and μ_0 is the permeability of free space. If only a single axis of the bearing is considered, then the net force acting on the shaft will be the difference of the two opposite acting actuator forces. Assuming the areas of the two opposing air gaps are the same, the force acting on the shaft by the magnetic bearing can be expressed as

$$F_{shaft} = \frac{1}{2\mu_0}(B_{g_1}{}^2 - B_{g_2}{}^2)A_g \qquad (2)$$

The flux density in the air gaps is being supplied by two sources, i.e., the permanent magnet and the coil. In order to properly provide differential control, the fluxes in the two gaps are symmetrically perturbed so that the flux in one gap is increased while the flux in the opposite gap is decreased by the same amount. This implies that

$$B_{g_1} = B_{pm} + B_c \text{ and } B_{g_2} = B_{pm} - B_c \tag{3,4}$$

where B_{pm} is the flux density generated by the permanent magnet and B_c is the flux density generated by the coil. Substituting Eqs. (3, 4) into Eq. (2), expanding and simplifying, the force acting on the shaft can now be expressed as

$$F_{shaft} = \frac{2}{\mu_0} B_{pm} B_c A_g \tag{5}$$

By expressing the equation for the force on the shaft in this form, it is interesting to note that the force is not only proportional to the bias level, B_{pm}, but it is also linearized with respect to the control flux, B_c.

Open Loop Stiffness and Actuator Gain

The force generated by the bearing in the horizontal direction, F_x, can be accurately approximated by the truncated Taylor series expansion in the following way:

$$F_x \approx F_x \Big|_{\substack{x=0 \\ i_c=0}} + \frac{\partial F}{\partial x}\Big|_{\substack{x=0 \\ i_c=0}} x + \frac{\partial F}{\partial i_c}\Big|_{\substack{x=0 \\ i_c=0}} i_c \tag{6}$$

If the magnetic circuit is balanced, then the first term in Eq. (6) is equal to zero and

$$F_x = K_x x + K_i i_c \tag{7}$$

where x represents the rotor displacement and i_c represents the control current in the electromagnetic coil. The parameters K_x and K_i are defined as

$$K_x \equiv \frac{\partial F_x}{\partial x}\Big|_{\substack{x=0 \\ i_c=0}} \text{ and } K_i \equiv \frac{\partial F_x}{\partial i_c}\Big|_{\substack{x=0 \\ i_c=0}} \tag{8,9}$$

The quantity K_x is referred to as the open loop stiffness and represents the change in the horizontal force due to horizontal displacement. The open loop stiffness is always negative which implies that the bearing is unstable in the open loop control configuration. Unlike a actual spring with a positive stiffness, a positive dispacement of the rotor toward the magnet will increase the attractive force. The quantity K_i represents the actuator gain of the bearing. It represents changes in the horizontal force due to control current, i_c. Equivalent expressions exist for the components of the vertical force expression. Expressions for the open loop stiffness and the actuator gain are determined by performing the appropriate differentiation of the force expression. These expressions take on the form

$$K_x = -\frac{2\mu_0 L^2 H^2 A_g}{g^3} \tag{10}$$

and

$$K_i = -\frac{\mu_0 LHNA_g}{g^2} \tag{11}$$

where L and H represent the length and demagnetization force, respectively, of the permanent magnet and N is the number of turns in the electromagnetic coil.

Control System Description

The control elements of this system are those components which detect the motion of the shaft, determine the required control force and generate a coil current required by the magnetic bearing to generate this force. The magnetic bearing system consists of four distinct components: the magnetic actuator, the displacement sensors and associated conditioning circuits, the analog PID controller and the power amplifier.

The actual magnetic bearing mainly consists of the electromagnetic coils, iron pole pieces, rotor and permanent magnets. The signal conditioning component consists of the eddy current induction displacement sensors, signal amplification and coordinate transformation circuits. The analog controller primarily consists of three separate components. The components take the form of proportional (P), integral (I) and derivative (D) compensation networks. These three parallel stages are added together through a summing amplifier to produce the output of the analog controller. The last component in the control loop is the power amplifier. The amplifier, upon request of the controller, supplies the required current to magnetic coils to produce the necessary fluxes in the bearing.

The dynamics of the bearing–rotor system can be combined with the operating characteristics of the control electronics to form a closed–loop control system. This control system is shown in a simplified block diagram form in Figure 3. The displacement sensor characteristics, analog controller and amplifier make up the relatively complex transfer function of the feedback controller, $G_c(s)$. The feedback controller relates the rotor position to the actuator current. The closed–loop transfer function for this magnetic bearing system, as determined from this block diagram, is given by

$$\frac{X(s)}{F_x(s)} = \frac{1}{ms^2 + K_x + K_i G_c(s)} \tag{12}$$

where m is the mass of the rotor supported by the bearing.

Prototype Bearing Construction

The four–pole radial bearing stators, as shown in the diagrams of Figures 1 and 2, were designed to be identical for both bearings. The stators and rotors were constructed of 3% silicon–iron lamination material which had a thickness of 0.007 inches. Each laminated component consists of approximately 100 laminations. The laminations were glued together using a two part activator/resin adhesive and the shape was machined by wire EDM (electric discharge machining.) The bearing stators have an outside diameter of approximately 3.0 inches and an

axial length of approximately 0.7 inches. The outside diameter of the laminated rotor is approximately 1.5 inches. The thrust bearing components were machined from soft magnet iron. The high energy permanent magnets, made out of a geodymium–Iron–Boron alloy, have a maximum energy product of 30 MG–Oe. The bearings support a shaft weighing approximately 3.7 lbm.

Load Capacity

Measurements of the maximum load applied to the shaft, before falling out of support, are plotted as a function of proportional controller gain, K_p, in Figure 4. The force in this test was applied by hanging weights on the shaft. A pulley system was constructed in such a way that the force could be applied in the desired direction. The force in the plots represents forces applied along the bearing axes.

The variation of the maximum load at lower proportional gains is actually a measure of the stability threshold of the system. It is noted in Eq. (8) that the open loop stiffness, K_x is defined at a nominal operating point, i.e., rotor position and control current equal to zero. However, as the bearing is loaded with a static force, the steady state current begins to increase. It can be shown analytically that K_x is a function of the operating point of the control current. That is, as the control current current increases, K_x also increases. Increasing proportional gain has the effect of compensating for this increase in K_x and consequently increasing the stability of the system.

The measurements made at higher proportional gains represent a more accurate measure of the actual load capacity of the bearing. Enough stability is provided so that magnetic saturation is reached in the bearing pole structures. The maximum predicted loads in the plots of Figure 4 are calculated at the point of magnetic saturation.

Equivalent Bearing Stiffness and Damping

Measurements of the equivalent stiffness of the bearings are shown in Figure 5. This simple measurement was performed by applying a constant force, ΔF , and noting the displacement, Δx , of the shaft (controller integrators turned off.) The stiffness then is given simply by $K_{eq} = \Delta F/\Delta x$. A linear regression was performed on the measured data, which resulted in very good correlation, as can be observed in the plots. It is noted that the proportional gain has a direct effect on the stiffness of the bearings, as has been previously demonstrated by Humphris, et. al. [11].

Relative damping in the bearings was investigated from a white noise frequency response analysis of the bearing and rotor. The analysis was performed by injecting noise, composed of all frequencies of interest, into one axis of the turbine–end radial bearing, and performing a FFT (Fast Fourier Transform) analysis on the vibration response of that axis. This linear frequency response, composed of 100 averages, is shown in Figure 6. The derivative controller gain, K_r was varied through a range of values as noted in the plot. As expected, the derivative gain had a direct effect on the damping in the bearings [11]. The first large spike represents the first two modes of shaft vibration. They are very close together in frequency and essentially indistinguishable. The frequency of the second spike is the third mode of vibration and the third small spike at approximately 60,000 cpm is the fourth mode. It is noted that the variation of the derivative gain strongly effects the first two modes, has a small effect on the third mode and virtually no influence on the vibration amplitude of the fourth mode.

Critical Speeds and Rotor Response

The damped synchronous critical speeds of the flexible shaft supported by these bearings can be approximately determined from the white noise frequency response plots of Figure 6. These values, however, represent the zero speed natural frequencies, and the gyroscopic stiffening effects of any attached disks would not be included. Since the natural frequency is given by $\omega_n = \sqrt{k/m}$, where k is the shaft stiffness and m in the modal mass of the rotor, it is of course expected that the observed critical speeds, when the shaft was spinning, would be higher.

Plots showing the vibration magnitude and phase for the shaft speeds that were obtained is included in Figure 7. Amplitude information was taken directly from the magnetic bearing sensors and a key–phase sensor was used to provide the phase information. According to the maximum vibration amplitudes observed in Figure 7, the first vibration mode is observed to occur at approximately 10,000 rpm and the second at approximately 13,000 rpm.

Power Consumption

Finally, a number of power consumption measurements were made. Measurements of the power were taken with a wattmeter for a number of cases. This meter is used with the assumption that the measured voltage and current being supplied to the control electronics is sinusoidal in nature. In addition, it is realized that it represents a somewhat gross measurement as it includes all the inefficiencies of the various electronic components. Table 1 summarizes the results. The non–essential electronic diagnostic components of the bearing system were observed to consume only about 7 watts. These measurements represent a significant improvement over the 500 watts of approximate total power consumed by a comparable current biased all electromagnetic bearing design.

CONCLUSIONS

The brief theory which was presented in this paper established the basic electromagnetic and mechanical relationships necessary to develop a set of permanent magnet biased magnetic bearings. The design involved both radial and thrust bearings. The availability of newer rare–earth high energy permanent magnets made it possible to effectively provide the necessary bias fluxes in the bearing.

The bearings and rotor were successfully constructed and operated. A number of tests and experiments were performed on the bearing–rotor system. The tests consisted of load capacity, stiffness and damping measurements. The results proved to be very positive in that the theoretical predictions and the observed performance matched reasonably well, giving credibility to the models which were used to perform the analysis. Of particular interest for this study was the measured power consumption of the bearings. It clearly demonstrates that the use of permanent magnets can improve the operating efficiency of an active magnetic bearing.

It was successfully observed and demonstrated that these bearings have strong potential for future use as efficient, reliable bearings. However, further research and development is required in the areas of controls, magnetic materials and actuator design before it is possible to install them into a useful industrial application.

REFERENCES

1. Allaire P.; Imlach, J.; McDonald, J.; Humphris, R.; Lewis, D.; Banerjee, B.; Blair, B.; Clayton, J.; Flack, R.: "Design, Construction and Test of Magnetic Bearings in an Industrial Canned Motor Pump," Pump Users Symposium, Texas A & M, Houston, TX, May 1989.

2. Weise, D. A.: "Present Industrial Applications of Active Magnetic Bearings," Presented at the 22nd Intersociety Energy Conversion Engineering Conference, Philadelphia, Pennsylvania, August 1987.

3. Burrows, C. R., Sahinkaya, N.; Traxler, A.; and Schweitzer, G.: "Design and Application of a Magnetic Bearing for Vibration Control and Stabilization of a Flexible Rotor," Proceedings of the First International Magnetic Bearings Symposium, ETH Zurich, Switzerland, June 1988.

4. Keith F. J., Williams, R. D.; Allaire, P. E.; and Schafer, R. M.: "Digital Control of Magnetic Bearings Supporting a Multimass Flexible Rotor," Presented at the Magnetic Suspension Technology Workshop, Hampton, Virginia, February 1988.

5. Studer. P. A.: NASA, Magnetic Bearing, Patent 3865442, Patent Application 100637, February 1975.

6. Studer, P. A.: NASA, Linear Magnetic Bearing, Patent 4387935, Patent Application 214361, December 1980.

7. Wilson, M.; and Studer, P. A.: "Linear Magnetic Bearings," Presented at the International Workshop on Rare Earth–Cobalt Magnets and Their Applications, Roanoake, Virginia, June 1981.

8. Ohkami, Y., Okamato, O.; Kida, T.; Murakami, C.; Nakajima, A.; Hagihara, S.; and Yabuuchi, K.: "A Comparison Study of Various Types of Magnetic Bearings Utilizing Permanent Magnets," Presented at the International Workshop on Rare Earth–Cobalt Permanent Magnets and Their Applications, Roanoake, Virginia, June 1981.

9. Tsuchiya, K; Inoue, M.; Nakajima, A.; Ohkami, Y.; and Murakami, C.: "On Stability of Magnetically Suspended Rotor at High Rotational Speed,." Presented at the Aerospace Sciences Meeting, Reno, Nevada, January 1989.

10. Meeks, C.: "Trends in Magnetic Bearing Design," Paper presented at Naval Sea Systems Command Magnetic Bearing Forum, Washington, D. C., July 1989.

11. Humphris, R. R.; Kelm, R. D.; Lewis, D. W.; and Allaire, P. E.: "Effect of Control Algorithms on Magnetic Journal Bearing Properties," *Journal of Engineering for Gas Turbines and Power*, Vol. 108, October 1986.

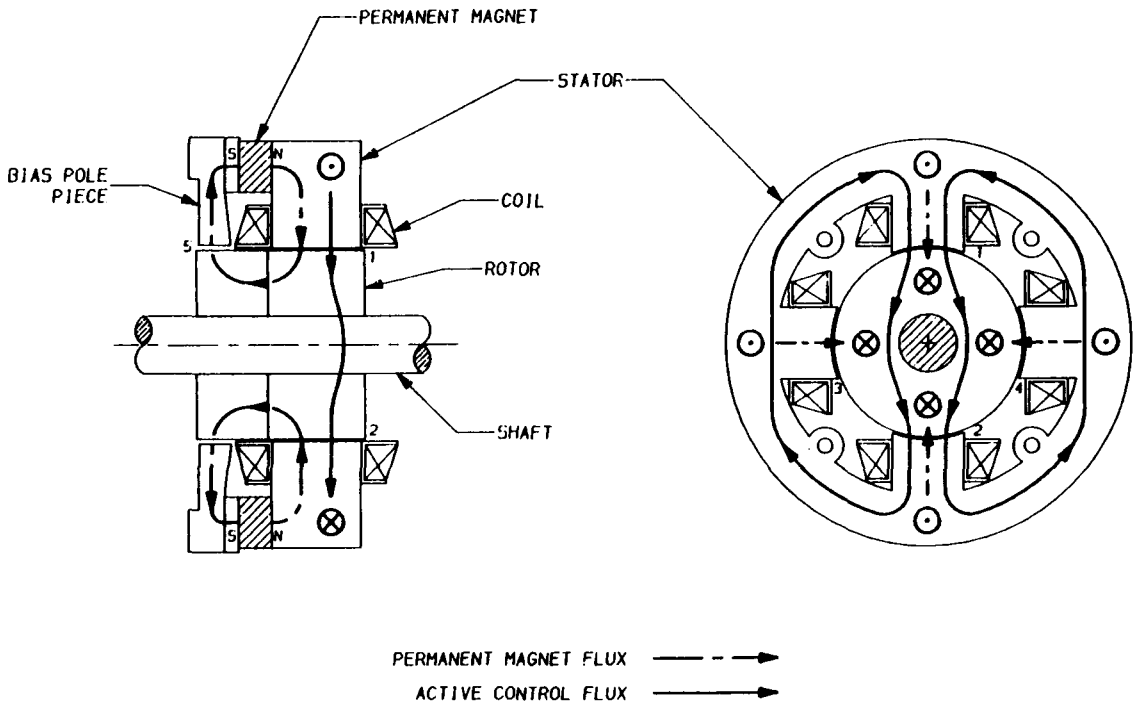

Figure 1 – Permanent Magnet Biased Radial Magnetic Bearing Flux Paths

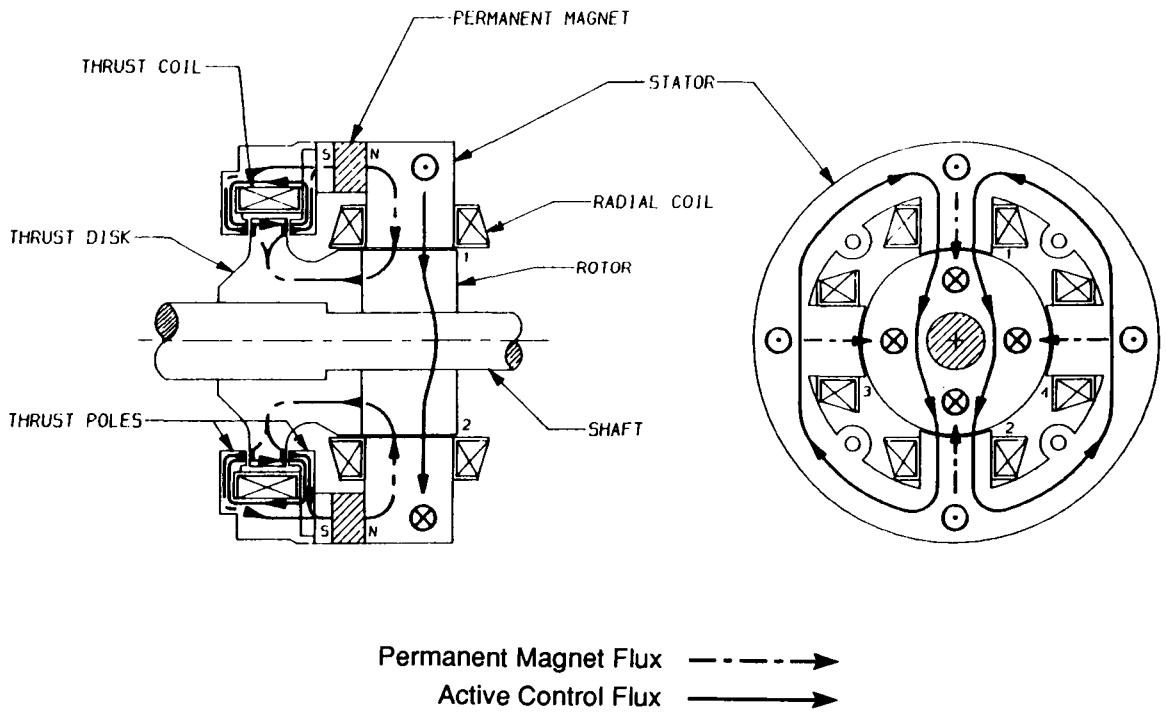

Figure 2 – Permanent Magnet Biased Radial/Thrust Magnetic Bearing Flux Paths

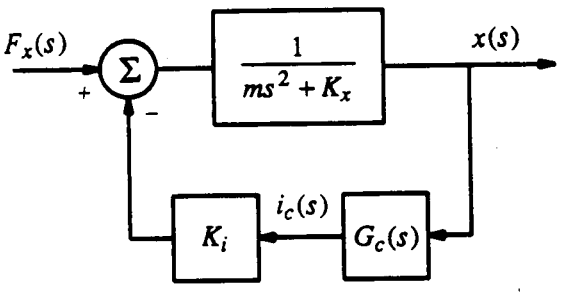

Figure 3 – Closed–Loop Magnetic Bearing Control System

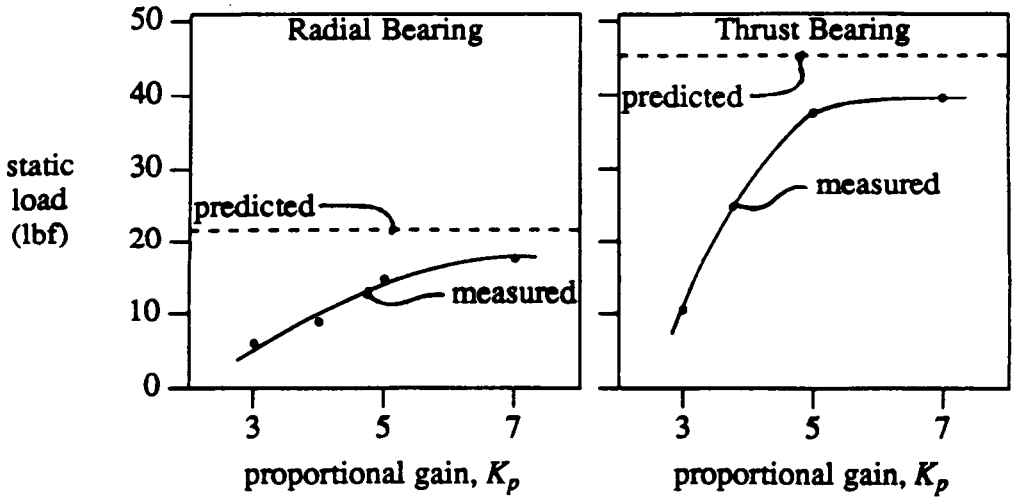

Figure 4 – Maximum Load Capacity

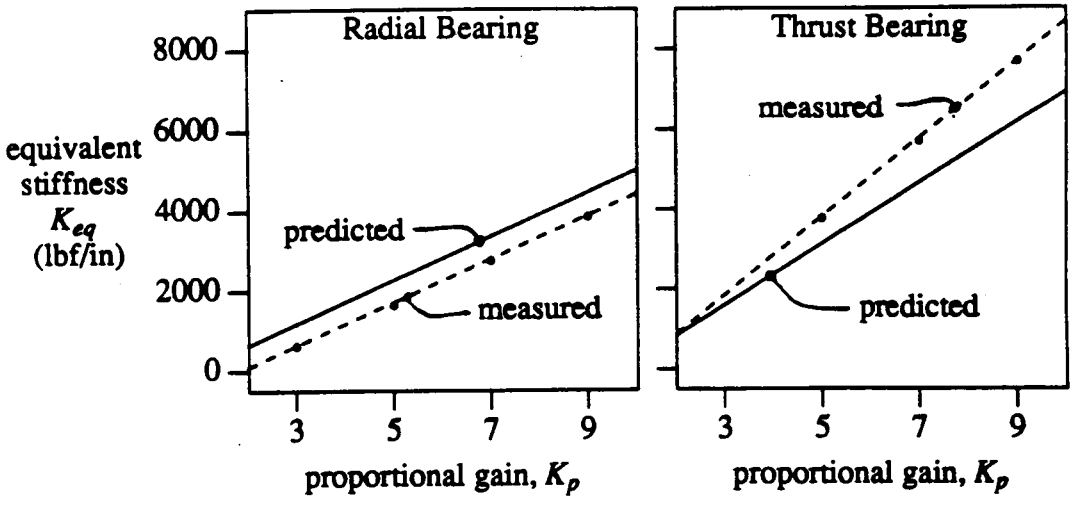

Figure 5 – Equivalent Bearing Stiffness

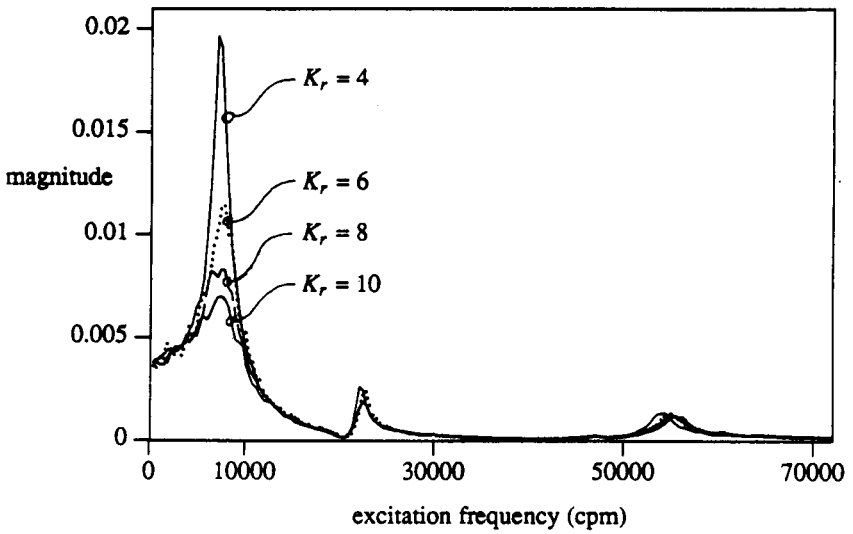

Figure 6 – Measured White Noise Linear Frequency Response

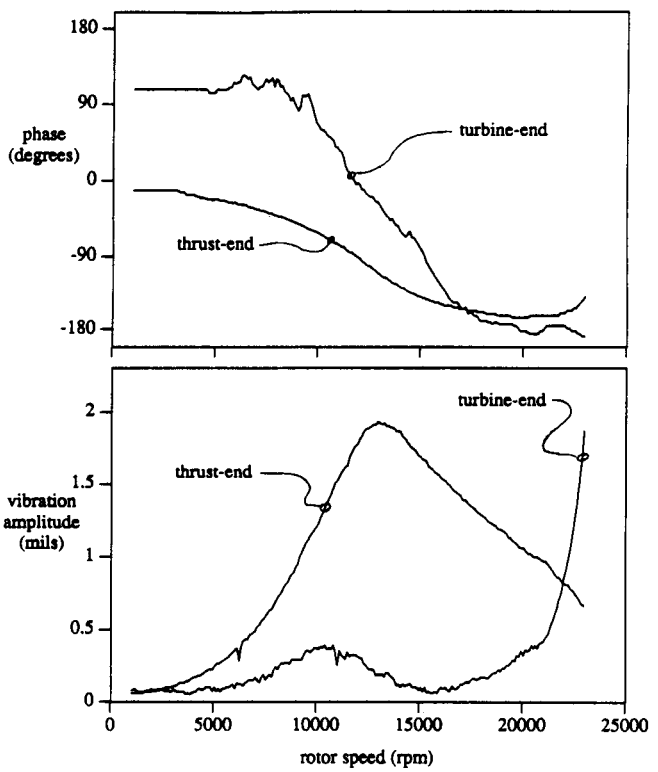

Figure 7 – Rotor Runup Response